Zygote **26** (June), pp. 224–231. © Cambridge University Press 2018
doi:10.1017/S0967199418000138 First Published Online 3 July 2018

Human cumulus cell sensitivity to vitrification, an ultrastructural study

Neda Taghizabet[2], *Mohammad Ali Khalili*[2], *Fatemeh Anbari*[2], *Azam Agha-Rahimi*[2], *Stefania Annarita Nottola*[3], *Guido Macchiarelli*[4] *and Maria Grazia Palmerini*[1]

Research and Clinical Center for Infertility, Shahid Sadoughi University of Medical Sciences, Yazd, Iran; Department of Anatomy, Histology, Forensic Medicine and Orthopaedics. University of Rome La Sapienza, Rome, Italy; and Department of Life, Health and Environmental Sciences, University of L'Aquila, L'Aquila, Italy

Date submitted: 13.02.2018. Date revised: 31.03.2018. Date accepted: 20.04.2018

Summary

Cumulus cells (CCs) play an important role in the regulation of female gamete development, meiotic maturation, oocyte–sperm interaction, capacitation and acrosome reaction. However, their role in maintaining oocyte competence after vitrification is unclear as controversial data on their protecting action against oocyte cryoinjuries are available. Here we described the effects of vitrification on the ultrastructure of human CCs collected from women undergoing assisted reproductive technologies (ARTs). In total, 50 patches of CCs, sampled from high-quality human cumulus–oocyte complexes, were randomly allocated into two groups after patient informed consent: 1, fresh CCs (controls, $n = 25$); 2, vitrified CCs ($n = 25$). Samples were then prepared and observed by transmission electron microscopy. In fresh CCs, in which small cell clusters were visible, cell membranes were joined by focal gap junctions. Microvilli were rare and short. Nuclei, mitochondria, smooth endoplasmic reticulum (SER), Golgi apparatus and lipid droplets appeared well preserved; vacuoles were scarce. After vitrification, we observed two populations of CCs: light CCs, with a smooth appearance and few short microvilli; and dark CCs, with numerous and long microvilli. In both, most of the organelles appeared similar to those of fresh CCs. Lipid droplets were denser and more numerous, with respect to fresh CCs. They were mainly located in the peri-nuclear and sub-plasmalemmal regions. Numerous packed electron-negative vacuoles were visible. The vitrification procedure did not cause alterations in the fine structure of major organelles, except for an increased amount of lipid droplets and vacuoles. This specific sensitivity of human CCs to vitrification should be considered during ARTs.

Keywords: ARTs, Cumulus cells, Human, TEM, Vitrification

Introduction

Vitrification of mature oocytes is routinely adopted in human clinics and research laboratories, even if with suboptimal yields. Among the numerous variables that can still be optimized, the role of cumulus cells (CCs) during vitrification has not fully elucidated. Data in the literature are controversial, evidencing a protecting role of CCs against oocyte cryoinjuries in some species or a barrier effect against the proper penetration of cryoprotectants in others. The extent of cryoinjuries depends, in fact, on factors including size and shape of the cells, membrane permeability, and oocyte quality and sensitivity. Indeed, all these factors may be highly variable depending on the species, developmental stage and origin (for example, *in vitro* produced or *in vivo* derived) (Vajta & Kuwayama, 2006).

In humans, mature oocytes showed significantly higher survival, cleavage and high-quality embryo

[1]All correspondence to: Maria Grazia Palmerini. Tel: +39 0862 433650. Fax: +39 0862 433523. E-mail: mariagrazia.palmerini@univaq.it
[2]Research and Clinical Center for Infertility, Shahid Sadoughi University of Medical Sciences, Yazd, Iran.
[3]Department of Anatomy, Histology, Forensic Medicine and Orthopaedics. University of Rome La Sapienza, Rome, Italy.
[4]Department of Life, Health and Environmental Sciences, University of L'Aquila, L'Aquila, Italy.

rates when CCs were retained with the oocytes before freezing (Jin *et al.*, 2012). In mice, mature oocytes vitrified with the surrounding cumulus cells (COCs, cumulus–oocyte complexes) were fertilized *in vitro* more efficiently than vitrified denuded oocytes (DOs) (Kohaya *et al.*, 2011). Fertilizability preservation was undoubtedly proved by the same group that recently obtained live rats from vitrified COCs fertilized *in vitro* with cryopreserved sperm (Fujiwara *et al.*, 2017). Similarly, vitrified immature mouse oocytes had higher survival, maturation and embryo developmental rates, with respect to the denuded vitrified counterpart (Nikseresht *et al.*, 2015). CCs also seemed to maintain the fertilization ability in vitrified bovine oocytes, as demonstrated by comparing blastocyst formation and cleavage rates from vitrified DOs and COCs. Both were significantly higher in vitrified multilayered COCs that, after IVF, successfully produced calves (Ishii *et al.*, 2018). Conversely, others found lower survival rates in vitrified bovine COCs, with respect to fresh and denuded oocytes, even if cleavage, blastocyst and fertilization rates were higher in vitrified COCs than in DOs (Ortiz-Escribano *et al.*, 2016). These might be explained by considering results previously obtained in sheep, in which the complete removal of CCs before vitrification enhanced oocyte survival and meiotic competence but impaired the activity of proteins such as maturation-promoting factor (MPF) and mitogen-activated protein kinase (MAPK) that could affect the developmental competence of oocytes (Bogliolo *et al.*, 2007). Higher fertilization rates found in the presence of CCs can be accounted for by their action in the prevention of zona hardening and maintenance of cortical granule number, as observed in humans using electron microscopy (Tong *et al.*, 2012).

Transmission electron microscopy (TEM) is the gold standard in revealing the microtopography and the ultrastructural characteristics of the cells and, indeed, is a tool in assessing the presence and extent of alterations connected to vitrification. To our knowledge, clinical outcomes and biomolecular data available are not yet sustained by a morphological evaluation on CCs exposed or not to vitrification, and are necessary to better identify the cryosensistivity of these cells in order to corroborate or disprove the theory of a protecting role of CCs against cryoinjuries. Therefore, to better clarify if cryoprotectants might affect the integrity of CCs in humans, we report in this study our ultrastructural observations made by TEM on discarded patches of CCs isolated from high-quality COCs that were recovered by women undergoing intracytoplasmic sperm injection (ICSI) due to male infertility factor and vitrified/thawed by CryoTop. Fresh CCs were used as controls.

Materials and Methods

Chemicals

All materials were purchased from Sigma Chemical Co. (St. Louis, MO, USA), unless stated otherwise.

Source of CCs

In total, 50 patches of CCs were sampled from mature COCs, collected by ovum pick up from 30 women aged 25–40 years who were undergoing ICSI cycles due to male infertility factor at the Yazd Reproductive Sciences Institute. Among ARTs, the ICSI procedure was specifically selected as a unique source of discarded CCs, as they are routinely removed from high-quality COCs prior to subsequent oocyte injection (Mangoli *et al.*, 2018). Briefly, gonadotropin-releasing hormone (GnRH) antagonist stimulation protocols were used for all participants (Eftekhar *et al.*, 2013). Transvaginal oocyte aspiration was performed 36 h after the trigger injections. COCs were removed from the collection fluid using a sterile pipette and washed in G-IVF (VitroLife, Sweden). Patches of CCs were then isolated with insulin needles from high-quality COCs and washed twice with G-Mops-V1 (VitroLife). Denuded oocytes were assessed for nuclear maturity under a stereomicroscope (Olympus Co., Japan) and used for patient treatment. Surplus CC patches were randomly divided into two groups: 1, fresh CCs (controls, $n = 25$); and 2, vitrified CCs ($n = 25$).

Vitrification and thawing

CCs were frozen utilizing a modified vitrification method (Al-Hasani *et al.*, 2007). The cells were equilibrated in a solution composed of 7.5% ethylene glycol (EG, Merck Co., Germany), 7.5% dimethyl sulphoxide (DMSO, Merck Co, Germany) in Ham's F10 medium supplemented with 20% human serum albumin (HSA, Plasbumin Co., USA) for 10 min at room temperature (RT). CCs were then transferred to a vitrification solution containing 15% EG, 15% DMSO and 0.5 M sucrose (Sigma Co., USA) in Ham's F10 medium supplemented with 20% HSA for 1 min at RT. The cells were then loaded on a CryoTop in a volume < 1 µl, and immediately immersed into liquid nitrogen (LN_2) for storage. For thawing, the cryotops were directly submerged into pre-incubated Ham's F10, 20% HSA and 1 M sucrose solution for 1 min the next day. Finally, the thawed CCs were rehydrated in Ham's F10 and 20% HSA (v/v) containing 0.5 or 0.25 M sucrose at RT for 3 and 5 min, respectively. The samples were finally rinsed in Ham's F10 and 20% HSA three times.

https://doi.org/10.1017/S0967199418000138 Published online by Cambridge University Press

Transmission electron microscopy

From each group, 15 CC samples were fixed and processed for TEM as previously reported (Bianchi *et al.*, 2014; Familiari *et al.*, 1998; Macchiarelli *et al.*, 2013; Nottola *et al.*, 2006, 2016; Palmerini *et al.*, 2014a, 2014b; 2017; 2018). Briefly, CCs were fixed for 2–5 days in 2.5% glutaraldehyde (Agar Scientific, Cambridge Road Stansted Essex, UK)/PBS at 4°C, embedded in 1% agar, then post-fixed with 1% osmium tetroxide (SIC, Rome, Italy). The samples were dehydrated in increasing concentrations of ethanol and then immersed in propylene oxide for solvent substitution. CC patches were individually embedded in EMbed-812 (Electron Microscopy Sciences, 1560 Industry Road, Hatfield, PA, USA). In the next step, the CCs were sectioned for light and electron microscopy observations. The cells were sectioned using a Reichert-Jung Ultracut E ultramicrotome (Reichert Technologies, Munich, Germany) at a thickness of 0.5–1 μm for light microscopy and stained with toluidine blue. Ultrathin sections of 60–80 nm were cut with a diamond knife, mounted on copper grids, and contrasted with saturated uranyl acetate and lead citrate (SIC, Rome, Italy) before being examined and photographed using Zeiss EM10 and Zeiss EM900 electron microscopes (Germany) operating at 80 kV.

The following parameters were evaluated by TEM and used in the qualitative assessment of CCs: general features; cell membrane integrity; characteristics of the nucleus, chromatin, and nuclear envelope; type and quality of organelles and inclusions; and presence and extent of cytoplasmic vacuolization (Nottola *et al.*, 2006; 2016).

ImageJ software (http://rsbweb.nih.gov/ij/) was used to measure cell dimension on low magnification TEM micrographs of control and vitrified CCs. For each experimental group, at least 15 CCs were selected for morphometric analysis.

Statistical analysis

All data were expressed as means ± standard deviation (SD). Statistical comparisons were performed using an unpaired *t*-test (GraphPad InStat). Differences in values were considered significant if *P*-values were <0.05.

Results

Group 1 (fresh CCs)

Fresh CCs [14.43 μm ± 0.874 μm, medium diameter ± standard deviation (SD)] showed a normal ultrastructure. Most of the CCs were round or oval and delimited by a continuous cytoplasmic membrane, occasionally protruding in short microvilli. Clustered cells showed small linear gap junctions (Fig. 1*a*). Large oval nuclei, with one or more nucleoli, were delimited by a continuous and electron-dense nuclear membrane (Fig. 1*a*). Spots of heterochromatin were clustered beneath the nuclear membrane (Fig. 1*a*). The organelles were abundant and uniformly scattered in the cytoplasm. Major organelles were those typical of steroidogenic cells as mitochondria, smooth endoplasmic reticulum (SER), Golgi apparatus and lipid droplets (Fig. 1*a*). Mitochondria appeared mainly ovoid or elongated, with numerous tightly packed tubulo-vesicular cristae (Fig. 1*b*). Tubular and vesicular SER elements were abundant and uniformly distributed throughout the cytoplasm (Fig. 1*c*). Cisternae and associated vesicles belonging to the Golgi apparatus were visible in the cytoplasm of fresh CCs. Numerous, spherical dark lipid droplets occupied the cytoplasm of fresh CCs (Fig. 1*c*). Free ribosomes, occasional lysosomes and electron-lucent vacuoles, sometimes containing debris, were also present (Fig. 1*c*).

Group 2 (vitrified CCs)

By TEM, vitrified CCs appeared mainly spherical (12.29 μm ± 0.701 μm, medium diameter ± SD; Group 2 versus Group 1: $P > 0.05$), isolated and delimited by a continuous cytoplasmic membrane (Fig. 2*a*). We observed two populations of CCs: light CCs had a smooth appearance, with a few short microvilli; in dark CCs the plasma membrane folded into numerous and long microvilli (Fig. 2*a–c*). The ratio nucleus/cytoplasm was occasionally higher respect what observed in fresh CCs (Fig. 2*a*, *c*). The nucleoplasm contained dispersed chromatin with one or more nucleoli, except for peripheral patches of heterochromatin, found attached to the inner leaflet of the nuclear membrane (Fig. 2*a*). The cytoplasm appeared populated with different types of organelles, with some differences with respect to group 1 (Fig. 2*b*). Organelles as mitochondria, tubular and vesicular elements of the SER and Golgi apparatus and ribosomes did not show significant variations with respect to Group 1. Lipid droplets were more numerous and larger than in fresh CCs in the 33.3% of vitrified patches and were packed around the peripheral cytoplasm or located in proximity of the nucleus, often close to elements of the endoplasmic reticulum (Fig. 2*a–c*).

Compared with group 1, in the 20% of vitrified patches the cytoplasm presented numerous large and clear vacuoles (Fig. 2*a*, *c*). In 40% of the observed 251 patches a concomitant increase in vacuoles and lipid droplets was found, while 6.7% of samples were mostly similar to the fresh controls.

https://doi.org/10.1017/S0967199418000138 Published online by Cambridge University Press

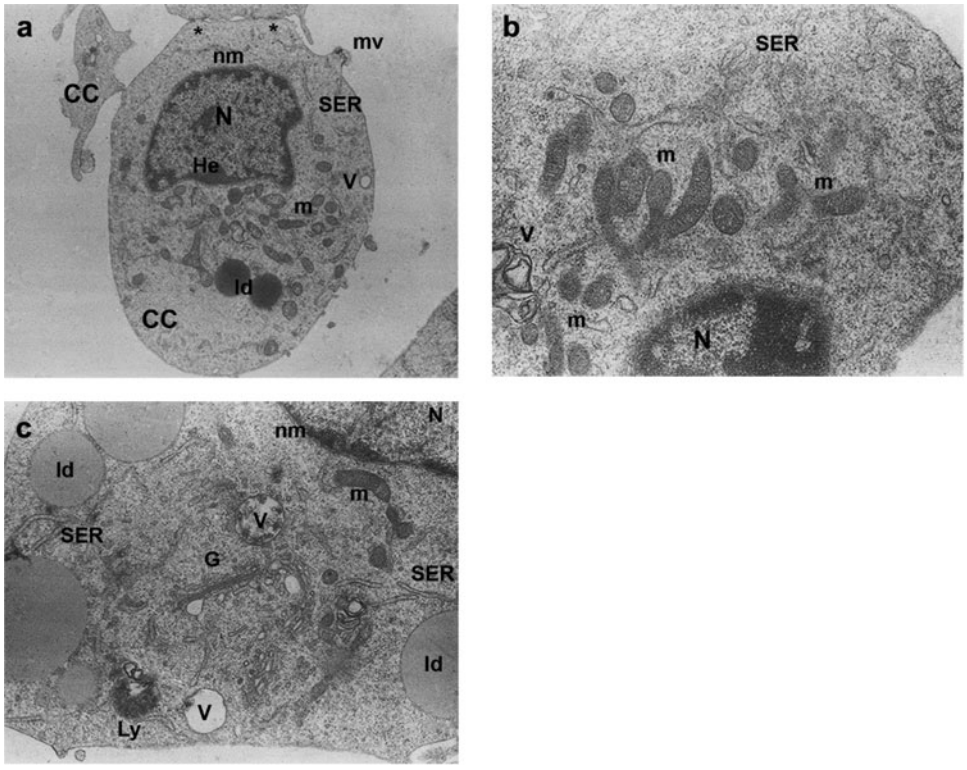

Figure 1 Fresh cumulus cells. (*a*) Representative micrograph of a fresh ovoidal-shaped human cumulus cell (CC), showing a nucleus (N) delimited by a continuous nuclear membrane (nm) and containing eccentric patches of heterochromatin (He). Cytoplasmic content is mainly constituted by numerous round-to-ovoid mitochondria (m), smooth endoplasmic reticulum (SER), electron-dense lipid droplets (ld). Rare microvilli (mv) are short and thin. Asterisks: Focal cell junctions between adjacent CCs. Transmission electron microscopy, ×9000 magnification. (*b*) At higher magnification ovoid or roundish mitochondria (m) show numerous stacked tubule-vesicular cristae. Numerous SER elements are visible near mitochondria. N: nucleus; V: vacuoles; CC: cumulus cell. Transmission electron microscopy, ×12,000 magnification. (*c*) The cytoplasm shows tubular and vesicular stacks of the Golgi apparatus (G), electron-dense lipid droplets (ld) delimited by a continuous membrane, SER elements, occasional lysosomes (Ly) and vacuoles (V), sometimes with electron-dense content. N: nucleus; m: mitochondria, nm: nuclear membrane. Transmission electron microscopy, ×12,000 magnification.

Discussion

CCs are known to be nourishing cells providing the supply of nutrients and signalling molecules through gap junctions and paracrine factors, necessary to sustain oocyte maturation. CCs also produce adhesive proteins useful to favour oocyte pick up and oviductal transport (Familiari *et al.*, 1996). In addition, they actively participate in the spermatozoa selection for a successful fertilization (Nottola *et al.*, 1998; Huang & Wells, 2010; Coticchio *et al.*, 2015; Zhou *et al.*, 2016; references therein). CCs may even have a role in positively affecting the microenvironment in which fertilization and early embryo development occur, both *in vivo* and *in vitro*, by producing small amounts of estrogens and progesterone, as revealed by their ultrastructure (Nottola *et al.*, 1991; Motta *et al.*, 1995).

In clinical practice, CCs are usually mechanically or enzymatically removed from COCs, to ascertain the meiotic stage of the oocyte before subsequent ARTs. When CCs are retained with the oocyte to ensure full developmental competence, there is the possibility that cryopreservation of COCs may compromise the functional coupling between oocyte and CCs, as seen in immature feline COCs (Luciano *et al.*, 2009) and in immature and mature porcine COCs (Wu *et al.*, 2006). Noteworthily, in equine immature COCs, vitrification induced the death of CCs invariably at the periphery of the cumulus layers, without compromising gap junction function or the ability of the oocytes to complete nuclear maturation (Tharasanit *et al.*, 2009). In humans, data present in the literature are controversial, with a group reporting that the denudation determined a significantly higher incidence of post-thaw meiotic spindle visualization and survival rates in DOs, when compared with COCs (Minasi *et al.*, 2012); another showing higher survival, cleavage and high-quality embryo rates when CCs were retained with the oocytes before freezing (Jin *et al.*, 2012) and a third that did not evidence any ultrastructural damage

https://doi.org/10.1017/S0967199418000138 Published online by Cambridge University Press

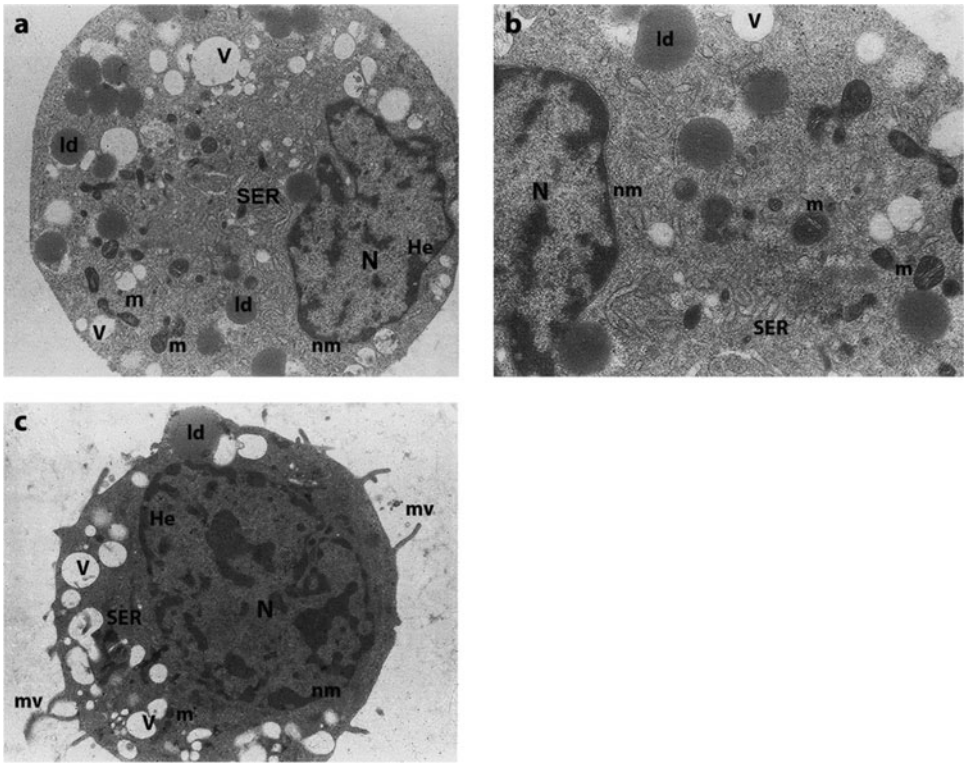

Figure 2 Vitrified cumulus cells. (*a*) A representative micrograph of a vitrified light human cumulus cells (CC), showing a nucleus (N) delimited by a continuous nuclear membrane (nm), irregularly folded and containing peripheric patches of heterochromatin (He). The cytoplasmic membrane appears smooth. The cytoplasmic content is constituted of numerous round-to-ovoid mitochondria (m) and smooth endoplasmic reticulum (SER). Numerous electron-negative vacuoles (V) occupy a pericortical or perinuclear position, often near lipid droplets (ld). Transmission electron microscopy, ×10,000 magnification. (*b*) Detail showing the close association between the tubular elements of the smooth endoplasmic reticulum (SER) and lipid droplets (ld). Transmission electron microscopy, ×12,000 magnification. (*c*) A vitrified dark human cumulus cell, characterized by a round profile with numerous long and thin microvilli (mv). A large nucleus (N), containing spots of heterochromatin (He) under the nuclear membrane (nm), occupies the largest portion of the CC. The high nucleus/cytoplasm ratio is probably an artefact due to the level of section. Numerous wide and clear vacuoles (V) are present in the cortical cytoplasm. Among these, mitochondria (m), tubular elements of the smooth endoplasmic reticulum (SER) and lipid droplets (ld) are dispersed. Transmission electron microscopy, ×9000 magnification.

or difference in the clinical outcomes between fresh controls, vitrified COCs and vitrified DOs, except for a higher fertilizing capability in vitrified COCs subjected to conventional IVF (Tong *et al.*, 2012). Overall, as we previously reported (Khalili *et al.*, 2017), the most cryo-sensitive structures of the human oocytes are microvilli, mitochondria, vacuoles and cortical granules with obvious specific differences between immature and mature oocytes, due to the presence of the nucleus and to the absence of the meiotic spindle in the formers.

To further clarify the role of CCs during vitrification in human, we aimed to analyze the ultrastructure of human CCs discarded from high-quality COCs undergoing ICSI, due to male infertility factor.

After vitrification, some CC cells showing a slightly dark cytoplasm and an irregular profile were found, with the plasma membrane folded into numerous and long microvilli. These cells resemble those belonging to a peculiar CC cell sub-population that, *in vivo*, appears specifically involved in sperm selection through phagocytosis (Pereda & Coppo, 1984; Motta *et al.*, 1995; Nottola *et al.*, 1998). Probably, the vitrification process induces a sort of 'hyperactivation' in some CC cells, with the expression of ultrastructural markers such as membrane irregularities and evaginations. Nuclear and cytoplasmic characteristics of these CC cells, however, are similar to those shown by the other CC cells and, at least in part, superimposable to those of fresh CCs, as reported below.

Intercellular connections were identified only in occasional clusters of fresh CCs, in which small linear gap junctions were observed. The absence of evident cell-to-cell interactions in vitrified CCs seems in contrast with the features shown by fresh or vitrified ovarian tissues, in which neighbouring cells

https://doi.org/10.1017/S0967199418000138 Published online by Cambridge University Press

maintained the established contacts after cryopreservation (Keros *et al.*, 2009; Nottola *et al.*, 2011; Sheikhi *et al.*, 2011). This discrepancy can be surely due to the use of expanded CCs that, after vitrification, thawing and the subsequent preparative for TEM observations are clearly more subjected to isolation.

After vitrification, even if the ratio of nucleus/cytoplasm appeared higher with respect to what was observed in fresh samples, CCs showed well preserved nuclei, as demonstrated by the presence of a continuous nuclear membrane, with patches of condensed chromatin attached on its inner leaflet. In our study, these features are comparable with those shown by the fresh counterpart. Similar characteristics are also observable in fresh COCs and vitrified human ovarian tissues containing metabolically active cells (Nottola *et al.*, 1998; Mazoochi *et al.*, 2008; Keros *et al.*, 2009; Sheikhi *et al.*, 2011).

Morphology of organelles in vitrified–thawed samples as mitochondria, SER elements, Golgi apparatus and ribosomes did not differ with respect to controls, in agreement with previous data from cryopreserved ovarian tissue (Salehnia *et al.*, 2002; Sheikhi *et al.*, 2011 and Keros *et al.*, 2009). Pleomorphic mitochondria, of different size and shape and containing tubular or vesicular cristae, were a typical feature of luteinizing CCs, concomitantly with a rich SER network and a well developed Golgi apparatus (Motta *et al.*, 2003).

Major ultrastructural differences between fresh and vitrified CCs involved lipid droplets and vacuoles. In our study, the 33.3% of vitrified patches of CCs showed an increased amount of electron-dense lipid droplets in the cytoplasm, centrally or eccentrically packed, in respect to those found in fresh CC. Accumulation of lipids, with the help of specific cytoskeletal activity allowing their compartmentalization, is one of the early signs of luteinization (Motta *et al.*, 1995). However, physical change of lipids at freezing temperature is one of the major causes of cellular cryodamage (Zhou & Li, 2013) and, therefore, our data confirmed the cryosensitivity of CCs against freezing, probably due to the used cryoprotectants (Fu *et al.*, 2009; Tayefi Nasrabadi *et al.*, 2015).

The sensitivity of CCs to vitrification was further demonstrated by an increased vacuolization found in the 20% of the vitrified patches and in the 40% of patches with the concomitant presence of increased lipid droplets. This finding is in agreement with other studies on human and mouse tissues (Salehnia *et al.*, 2002; Keros *et al.*, 2009) but in contrast with one study on vitrified human ovarian tissue, in which granulosa cells showed uniform contact with no obvious increase in the level of vacuolization (Sheikhi *et al.*, 2011). These data could be a probable consequence of the stepwise vitrification method used in this former study. It should be noted that the appearance of vacuoles is considered a non-specific response to cryodamage or osmotic stress (Khalili *et al.*, 2012) that may also occur in human oocytes cryopreserved using different protocols of slow freezing or vitrification (Palmerini *et al.*, 2014a; Nottola *et al.*, 2016; Khalili *et al.*, 2012; 2017).

In conclusion, the data obtained in the present study highlighted the effect of vitrification on the ultrastructure of CCs collected from mature COCs taken from women who were undergoing ICSI.

We found that vitrification can preserve the fine structure of major organelles of human CCs. Nevertheless, an increase in lipid droplets and vacuoles was observed, thus confirming the cryosensitivity of these cells.

This study revealed that CC cell patches may be considered a simple and effective biological model to test cell damage during cryopreservation. In addition, based on our results, we can speculate that the maintenance of CCs around the oocyte during vitrification could decrease the extent of cryodamage to the oocyte, thus contributing to the preservation of oocyte competence for fertilization. Retained CCs could in fact create a sort of natural, protective shield around the oocyte against physico-chemical insults due to the cryopreservation procedure. Further studies are needed on vitrified COCs, if available, to have a complete, parallel view of both CC and oocyte ultrastructural morphology with the final aim of contributing to the optimization of the current vitrification protocols.

Financial support

This work was supported by the Department of Life, Health and Environmental Sciences, University of L'Aquila, Italy (RIA 2015–2018) and the Department of Anatomy, Histology, Forensic Medicine and Orthopaedics, La Sapienza University of Rome, Italy (University grants 2015–2017).

Conflicts of interest

None

Ethical standards

The Ethics Committee of Yazd Reproductive Sciences Institute, Shahid Sadoughi University of Medical Sciences, Yazd, Iran, approved this study (ethical code: IR. SSU. Medicine Rec. 1392.300). All experiments involving human participants were performed in

https://doi.org/10.1017/S0967199418000138 Published online by Cambridge University Press

accordance with the 1964 Helsinki declaration and relevant guidelines. Written informed consents were obtained from all patients who participated in our research study.

References

Al-Hasani, S., Ozmen, B., Koutlaki, N., Schoepper, B., Diedrich, K. & Schultze-Mosgau, A. (2007). Three years of routine vitrification of human zygotes: is it still fair to advocate slow-rate freezing? *Reprod. Biomed. Online* **14**, 288–93.

Bianchi, V., Macchiarelli, G., Borini, A., Lappi, M., Cecconi, S., Miglietta, S., Familiari, G. & Nottola, S.A. (2014). Fine morphological assessment of quality of human mature oocytes after slow freezing or vitrification with a closed device: a comparative analysis. *Reprod. Biol. Endocrinol.* **12**, 110.

Bogliolo, L., Ariu, F., Fois, S., Rosati, I., Zedda, M.T., Leoni, G., Succu, S., Pau, S. & Ledda, S. (2007). Morphological and biochemical analysis of immature ovine oocytes vitrified with or without cumulus cells. *Theriogenology* **68**, 1138–49.

Coticchio, G., Dal Canto, M., Mignini Renzini, M., Guglielmo, M.C., Brambillasca, F., Turchi, D., Novara, P.V. & Fadini, R. (2015). Oocyte maturation: gamete-somatic cells interactions, meiotic resumption, cytoskeletal dynamics and cytoplasmic reorganization. *Hum. Reprod. Update* **21**, 427–54.

Eftekhar, M., Aflatoonian, A., Mohammadian, F. & Eftekhar, T. (2013). Adjuvant growth hormone therapy in antagonist protocol in poor responders undergoing assisted reproductive technology. *Arch. Gynecol. Obstet.* **287**, 1017–21.

Familiari, G., Verlengia, C., Nottola, S.A., Renda, T., Micara, G., Aragona, C., Zardi, L. & Motta, P.M. (1996). Heterogeneous distribution of fibronectin, tenascin-C, and laminin immunoreactive material in the cumulus–corona cells surrounding mature human oocytes from IVF-ET protocols – evidence that they are composed of different subpopulations: an immunohistochemical study using scanning confocal laser and fluorescence microscopy. *Mol. Reprod. Dev.* **43**, 392–402.

Familiari, G., Verlengia, C., Nottola, S.A., Tripodi, A., Hyttel, P., Macchiarelli, G. & Motta, P.M. (1998). Ultrastructural features of bovine cumulus–corona cells surrounding oocytes, zygotes and early embryos. *Reprod. Fertil. Dev.* **10**, 315–26.

Fu, X.W., Shi, W.Q., Zhang, Q.J., Zhao, X.M., Yan, C.L., Hou, Y.P., Zhou, G.B., Fan, Z.Q., Suo, L., Wusiman, A., Wang, Y.P. & Zhu, S.E. (2009). Positive effects of Taxol pretreatment on morphology, distribution and ultrastructure of mitochondria and lipid droplets in vitrification of *in vitro* matured porcine oocytes. *Anim. Reprod. Sci.* **115(**1–4**)**, 158–68.

Fujiwara, K., Kamoshita, M., Kato, T., Ito, J. & Kashiwazaki, N. (2017). Generation of rats from vitrified oocytes with surrounding cumulus cells via *in vitro* fertilization with cryopreserved sperm. *Anim. Sci. J.* **88**, 180–4.

Huang, Z. & Wells, D (2010). The human oocyte and cumulus cells relationship: new insights from the cumulus cell transcriptome. *Mol. Hum. Reprod.* **16**, 715–25.

Ishii, T., Tomita, K., Sakakibara, H. & Ohkura, S. (2018). Embryogenesis of vitrified mature bovine oocytes is improved in the presence of multi-layered cumulus cells. *J. Reprod. Dev.* **64**, 95–9.

Jin, H.X., Song, W.Y., Xin, Z.M., Dai, S.J., Chen, Z.J. & Sun, Y.P. (2012). Effects of cumulus cells on vitreous cryopreservation of human mature oocytes and clinical pregnancy outcomes. *Reprod. Sci.* **19**, 216–20.

Keros, V., Xella, S., Hultenby, K., Pettersson, K., Sheikhi, M., Volpe, A., Hreinsson, J. & Hovatta, O. (2009). Vitrification versus controlled-rate freezing in cryopreservation of human ovarian tissue. *Hum. Reprod.* **24**, 1670–83.

Khalili, M.A., Maione, M., Palmerini, M.G., Bianchi, S., Macchiarelli, G. & Nottola, S.A. (2012). Ultrastructure of human mature oocytes after vitrification. *Eur. J. Histochem.* **56**, e38

Khalili, M.A., Shahedi, A., Ashourzadeh, S., Nottola, S.A., Macchiarelli, G. & Palmerini, M.G. (2017). Vitrification of human immature oocytes before and after *in vitro* maturation: a review. *J. Assist. Reprod. Genet.* **34**, 1413–26.

Kohaya, N., Fujiwara, K. & Ito, J., Kashiwazaki, N. (2011). High developmental rates of mouse oocytes cryopreserved by an optimized vitrification protocol: the effects of cryoprotectants, calcium and cumulus cells. *J. Reprod. Dev.* **57**, 675–80.

Luciano, A.M., Chigioni, S., Lodde, V., Franciosi, F., Luvoni, G.C. & Modina, S.C. (2009). Effect of different cryopreservation protocols on cytoskeleton and gap junction mediated communication integrity in feline germinal vesicle stage oocytes. *Cryobiology* **59**, 90–5.

Macchiarelli, G., Palmerini, M.G., Nottola, S.A., Cecconi, S., Tanemura, K. & Sato, E. (2013). Restoration of corpus luteum angiogenesis in immature hypothyroid RDW rats after thyroxine treatment: morphologic and molecular evidence. *Theriogenology* **79**, 116–26.

Mangoli, E., Khalili, M.A., Talebi, A.R., Ghasemi-Esmailabad, S. & Hosseini, A. (2018). Is there any correlation between sperm parameters and chromatin quality with embryo morphokinetics in patients with male infertility? *Andrologia* doi:10.1111/and.12997. [Epub ahead of print]

Mazoochi, T., Salehnia, M., Valojerdi, M.R. & Mowla, S.J. (2008). Morphologic, ultrastructural, and biochemical identification of apoptosis in vitrified-warmed mouse ovarian tissue. *Fertil. Steril.* **90**(4 Suppl), 1480–6.

Minasi, M.G., Fabozzi, G., Casciani, V., Ferrero, S., Litwicka, K. & Greco, E. (2012). Efficiency of slush nitrogen vitrification of human oocytes vitrified with or without cumulus cells in relation to survival rate and meiotic spindle competence. *Fertil. Steril.* **97**, 1220–5.

Motta, P.M., Nottola, S.A., Pereda, J., Croxatto, H.B. & Familiari, G. (1995). Ultrastructure of human cumulus oophorus: a transmission electron microscopic study on oviductal oocytes and fertilized eggs. *Hum. Reprod.* **10**, 2361–7.

Motta, P.M., Nottola, S.A., Familiari, G., Makabe, S., Stallone, T. & Macchiarelli, G. (2003). Morphodynamics of the follicular-luteal complex during early ovarian development and reproductive life. *Int. Rev. Cytol.* **223**, 177–288.

Nikseresht, M., Toori, M.A., Rasti, T., Kashani, I.R. & Mahmoudi, R. (2015). The nuclear maturation and embryo development of mice germinal vesicle oocytes with and

without cumulus cell after vitrification. *J. Clin. Diagn. Res.* **9**, AF01–4.

Nottola, S.A., Familiari, G., Micara, G., Aragona, C. & Motta, P.M. (1991). The ultrastructure of human cumulus–corona cells at the time of fertilization and early embryogenesis. A scanning and transmission electronmicroscopic study in an *in vitro* fertilization program. *Arch. Histol. Cytol.* **54**, 145–61.

Nottola, S.A., Macchiarelli, G., Familiari, G., Stallone, T., Sathananthan, A.H. & Motta, P.M. (1998). Egg–sperm interactions in humans: ultrastructural aspects. *Ital. J. Anat. Embryol.* **103**(4 Suppl. 1), 85–101.

Nottola, S.A., Heyn, R., Camboni, A., Correr, S. & Macchiarelli, G. (2006). Ultrastructural characteristics of human granulosa cells in a coculture system for *in vitro* fertilization. *Microsc. Res. Tech.* **69**, 508–16.

Nottola, S.A., Cecconi, S., Bianchi, S., Motta, C., Rossi, G., Continenza, M.A. & Macchiarelli, G. (2011). Ultrastructure of isolated mouse ovarian follicles cultured *in vitro. Reprod. Biol. Endocrinol.* **9**, 3.

Nottola, S.A., Albani, E., Coticchio, G., Palmerini, M.G., Lorenzo, C., Scaravelli, G., Borini, A., Levi-Setti, P.E. & Macchiarelli, G. (2016). Freeze/thaw stress induces organelle remodeling and membrane recycling in cryopreserved human mature oocytes. *J. Assist. Reprod. Genet*. **33**, 1559–70.

Ortiz-Escribano, N., Smits, K., Piepers, S., Van den Abbeel, E., Woelders, H. & Van Soom, A. (2016). Role of cumulus cells during vitrification and fertilization of mature bovine oocytes: effects on survival, fertilization, and blastocyst development. *Theriogenology* **86**, 635–41.

Palmerini, M.G., Antinori, M., Maione, M., Cerusico, F., Versaci, C., Nottola, S.A., Macchiarelli, G., Khalili, M.A. & Antinori, S. (2014a). Ultrastructure of immature and mature human oocytes after CryoTop vitrification. *J. Reprod. Dev.* **60**, 411–20.

Palmerini, M.G., Nottola, S.A., Leoni, G.G., Succu, S., Borshi, X., Berlinguer, F., Naitana, S., Bekmukhambetov, Y. & Macchiarelli, G. (2014b). *In vitro* maturation is slowed in prepubertal lamb oocytes: ultrastructural evidences. *Reprod. Biol. Endocrinol.* **12**, 115.

Palmerini, M.G., Zhurabekova, G., Balmagambetova, A., Nottola, S.A., Miglietta, S., Belli, M., Bianchi, S., Cecconi, S., Di Nisio, V., Familiari, G. & Macchiarelli, G. (2017). The pesticide Lindane induces dose-dependent damage to granulosa cells in an *in vitro* culture. *Reprod. Biol.* **17**, 349–56.

Palmerini, M.G., Belli, M., Nottola, S.A., Miglietta, S., Bianchi, S., Bernardi, S., Antonouli, S., Cecconi, S., Familiari, G. & Macchiarelli, G. (2018). Mancozeb impairs the ultrastructure of mouse granulosa cells in a dose-dependent manner. *J. Reprod. Dev.* **64**, 75–82.

Pereda, J. & Coppo, M. (1984). Ultrastructure of the cumulus cell mass surrounding a human egg in the pronuclear stage. *Anat. Embryol. (Berl.)* **170**, 107–12.

Salehnia, M., Abbasian Moghadam, E. & Rezazadeh Velojerdi, M. (2002). Ultrastructure of follicles after vitrification of mouse ovarian tissue. *Fertil. Steril.* **78**, 644–5.

Sheikhi, M., Hultenby, K., Niklasson, B., Lundqvist, M. & Hovatta, O. (2011). Clinical grade vitrification of human ovarian tissue: an ultrastructural analysis of follicles and stroma in vitrified tissue. *Hum. Reprod.* **26**, 594–603.

Tayefi Nasrabadi, H., Gavami, M., Akbarzadeh, A., Beheshti, R., Mohammadnejad, D. & Abedelahi, A. (2015). Preservation of mouse ovarian tissue follicle morphology and ultrastructure after vitrifying in biotechnological protocols. *J. Ovarian Res.* **8**, 7.

Tharasanit, T., Colleoni, S., Galli, C., Colenbrander, B. & Stout, T.A. (2009). Protective effects of the cumulus–corona radiata complex during vitrification of horse oocytes. *Reproduction* **137**, 391–401.

Tong, X.H., Wu, L.M., Jin, R.T., Luo, L.H., Luan, H.B. & Liu, Y.S. (2012). Fertilization rates are improved after IVF if the corona radiata is left intact in vitrified-warmed human oocytes. *Hum. Reprod.* **27**, 3208–14.

Vajta, G. & Kuwayama, M. (2006). Improving cryopreservation systems. *Theriogenology* **65**, 236–44.

Wu, C., Rui, R., Dai, J., Zhang, C., Ju, S., Xie, B., Lu, X. & Zheng, X. (2006). Effects of cryopreservation on the developmental competence, ultrastructure and cytoskeletal structure of porcine oocytes. *Mol. Reprod. Dev.* **73**, 1454–62.

Zhou, C.J., Wu, S.N., Shen, J.P., Wang, D.H., Kong, X.W., Lu, A., Li, Y.J., Zhou, H.X., Zhao, Y.F. & Liang, C.G. (2016). The beneficial effects of cumulus cells and oocyte–cumulus cell gap junctions depends on oocyte maturation and fertilization methods in mice. *Peer J.* **4**, e1761.

Zhou, G.B. & Li, N. (2013). Bovine oocytes cryoinjury and how to improve their development following cryopreservation. *Anim. Biotechnol.* **24**, 94–106.